

1
2
3
4
5
6
7
8
9
10
11
12
13
14
15
16
17
18
19
20
21
22
23
24
25
26
27
28
29
30
31
32
33
34
35
36
37
38
39
40
41
42
43
44
45
46
47
48
49
50
51
52
53
54
55
56
57
58
59
60
61
62
63
64
65

27 **SUMMARY**

28 Chronic kidney disease (CKD) increases fracture risk. The results of this work point to changes
29 in bone collagen and bone hydration as playing a role in bone fragility associated with CKD.

30

1
2
3
4
5
6
7
8
9
10
11
12
13
14
15
16
17
18
19
20
21
22
23
24
25
26
27
28
29
30
31
32
33
34
35
36
37
38
39
40
41
42
43
44
45
46
47
48
49
50
51
52
53
54
55
56
57
58
59
60
61
62
63
64
65

31 **ABSTRACT**

32 **Purpose/Introduction:** Clinical data have documented a clear increase in fracture risk
33 associated with chronic kidney disease (CKD). Preclinical studies have shown reductions in
34 bone mechanical properties although the tissue-level mechanisms for these differences remain
35 unclear. The goal of this study was to assess collagen cross-links and matrix hydration, two
36 variables known to affect mechanical properties, in animals with either high or low turnover
37 CKD. **Methods:** At 35 weeks of age (>75% reduction in kidney function), the femoral diaphysis
38 of male Cy/+ rats with high or low bone turnover rates, along with normal littermate (NL)
39 controls, were assessed for collagen cross-links (pyridinoline (PYD), deoxypyridinoline (DPD),
40 and pentosidine (PE)) using a high performance liquid chromatography (HPLC) assay as well as
41 pore and bound water per volume (pw and bw) using a ¹H nuclear magnetic resonance (NMR)
42 technique. Material-level biomechanical properties were calculated based on previously
43 published whole bone mechanical tests. **Results:** Cortical bone from animals with high turnover
44 disease had lower Pyd and Dpd crosslink levels (-21% each), lower bw (-10%), higher PE
45 (+71%), and higher pw (+46%), compared to NL. Animals with low turnover had higher Dpd, PE
46 (+71%), and bw (+7%) along with lower pw (-60%) compared to NL. Both high and low turnover
47 animals had reduced material-level bone toughness compared to NL animals as determined by
48 three-point bending. **Conclusions:** These data document an increase in skeletal PE with
49 advanced CKD that is independent of bone turnover rate and inversely related to decline in
50 kidney function. Although hydration changes occur in both high and low turnover disease, the
51 data suggest that non-enzymatic collagen crosslinks may be a key factor in compromised
52 mechanical properties of CKD.

1
2
3
4
5
6
7
8
9
10
11
12
13
14
15
16
17
18
19
20
21
22
23
24
25
26
27
28
29
30
31
32
33
34
35
36
37
38
39
40
41
42
43
44
45
46
47
48
49
50
51
52
53
54
55
56
57
58
59
60
61
62
63
64
65

57 INTRODUCTION

58 There are clear and consistent data showing that chronic kidney disease (CKD) is associated
59 with an increased fracture risk compared to individuals without CKD [1-5]. More concerning is
60 that individuals with CKD who experience a fracture are at greater risk of mortality compared to
61 people without CKD who fracture [6, 7]. There are numerous challenges to reducing fracture risk
62 in CKD patients because of the complexity in the underlying bone disease. CKD is associated
63 with significant metabolic derangements, including secondary hyperparathyroidism, yet some
64 patients have low levels of parathyroid (PTH) for unclear reasons [1, 8, 9]. At the skeletal level,
65 CKD appears to have a preferential impact on cortical bone, leading to increased porosity, and
66 likely playing a major role in fracture [10-14]. Preclinical studies have documented CKD-
67 associated reductions in biomechanical properties of whole bones, as well as at the micro- and
68 nano-scale levels of the hierarchical organization of bone [14-18]. Properties of the tissue, such
69 as mineral content, have not shown clear differences between normal and diseased bone
70 leaving a cloud of uncertainty as to what properties of the tissue are responsible for this
71 compromised mechanical phenotype associated with CKD [16].

72 Increased attention to 'bone quality' (those aspects other than BMD that account for a
73 bone's resistance to fracture) has led to a greater understanding of various skeletal properties
74 [19-21]. Collagen plays a vital role in bone with changes in collagen cross-links showing clear
75 influence on bone mechanical properties [22-26]. CKD-induced collagen changes have been
76 noted in serum and several soft-tissues [27] but data in bone are limited [28, 29]. A less often
77 discussed bone quality variable, bone hydration, also affect bone mechanical properties [30-32],
78 but only recently has it become clear that *in vivo* modulation of hydration can play a role in a
79 bone's fracture resistance capacity [33-35].

80 While there is an increasing awareness of the importance of bone quality in CKD [20,
81 21], few studies have explicitly examined material properties in animal models [14-16, 18, 29].
82 The goal of the present study was to examine two specific properties, collagen crosslinks and

1
2
3
4
5
6
7
8
9
10
11
12
13
14
15
16
17
18
19
20
21
22
23
24
25
26
27
28
29
30
31
32
33
34
35
36
37
38
39
40
41
42
43
44
45
46
47
48
49
50
51
52
53
54
55
56
57
58
59
60
61
62
63
64
65

83 matrix hydration (bound and pore water) in a rat model with progressive development of CKD
84 that can be manipulated to have either high or low turnover disease [14, 36]. We hypothesized
85 that CKD adversely affects both collagen cross-links and matrix hydration, that these
86 parameters would be most affected in high turnover disease, and there would be relationships
87 between these properties and bone mechanical outcomes.

88

89 **MATERIALS AND METHODS**

90 *Animal Model*

91 The current study utilized a slowly progressive animal model of CKD, the Cy/+ rat, which has
92 been described in detail several times [15, 16, 18, 36-38]. Tissues analyzed in the current study
93 were from select groups of animals that were part of a larger study [14]. Specifically, the
94 animals were in one of three groups: Cy/+ animals that were untreated and thus had high
95 turnover bone disease, Cy/+ given calcium supplementation in their drinking water to suppress
96 PTH starting at 25 weeks of age (low turnover disease), or normal littermate controls (n=8-
97 10/gp). All animals were euthanized at 35 weeks of age and femora (used to study both
98 outcome measures) were saved wrapped in saline soaked gauze at -20C. Prior to the assays
99 reported in this paper, femora were tested in 3 point bending [14]. Blood was also collected at
100 the end of the experiment for biochemical analyses. Dynamic histomorphometry (detailing
101 turnover rates), 3 point bending, and biochemical assays have all been previously reported [14].
102 All procedures were conducted under the approval of Indiana University School of Medicine
103 Institutional Animal Care and Use Committee protocol # 10479.

104

105 *Collagen Cross-Linking*

106 Segments of the femoral diaphysis (~3 mm in length) were processed for collagen cross-links
107 as previously described [16]. Briefly, following demineralized in 20% EDTA (0.68 M, pH 7.4),
108 demineralized bone was hydrolyzed. Each hydrolysate was resuspended in ultrapure water,

1
2
3
4 109 split into two equal portions, and dried. Half the residue was resuspended in ultrapure water with
5
6 110 an internal standard (5×10^{-6} g/L pyridoxine) and assayed by a high performance liquid
7
8 111 chromatography (HPLC) system (Beckman-Coulter System Gold 168). Standards with varying
9
10 112 concentrations of pyridinoline (Pyd) (Quidel), deoxypyridinoline (Dpd) (Quidel), pentosidine (PE)
11
12 113 (International Maillard Reaction Society), and a constant amount of pyridoxine were also
13
14 114 assayed. Using a Waters 2475 fluorescence detector (excitation/emission of 295/400 nm for
15
16 115 Pyd and Dpd and 328/378 nm for PE), chromatograms were recorded to determine the amount
17
18 116 of each crosslink. These amounts were then normalized by collagen content (hydroxyproline),
19
20 117 which was determined from the other half of each hydrolysate by another HPLC assay. The
21
22 118 calculated mass of hydroxyproline was then multiplied by 7.5 (assuming 13-14% of type I
23
24 119 collagen by mass) and divided by the molecular weight of collagen (30,000 Da), thereby giving
25
26 120 crosslink concentration as mol/mol of collagen. For each chromatogram, the area of the peak
27
28 121 is calculated and divided by an internal standard. These values are then plotted onto a standard
29
30 122 curve that plots the known masses of the standards to their given areas, providing an estimate
31
32 123 of the mass of the given molecule in the unknowns (hydroxyproline, pyridinoline,
33
34 124 deoxypyridinoline, and pentosidine).
35
36
37
38
39
40
41

42 126 *¹H Nuclear magnetic resonance spectroscopy (NMR)*

43
44

45 127 A ~5 mm cross-section of the femur mid-shaft was placed into a low proton, loop-gap-style
46
47 128 radio-frequency (RF) coil [39] along with a reference microsphere of water ($T_2 \sim 2$ s). The NMR
48
49 129 analysis to separate proton signals within the bone was then performed in a 4.7T horizontal-
50
51 130 bore magnet (Varian Medical Systems, Santa Clara, CA) using $90^\circ/180^\circ$ RF pulses of $\sim 9/18 \mu\text{s}$
52
53 131 duration and collecting Carr-Purcell-Meiboom-Gill (CPMG) measurements with 10,000 echoes
54
55 132 at $100 \mu\text{s}$ spacing. To generate the spectrum of transverse relaxation time constants (T_2), the
56
57 133 echo magnitudes were fitted with multiple exponential decay functions [40]. Upon normalizing
58
59
60
61
62
63
64
65

1
2
3
4
5
6
7
8
9
10
11
12
13
14
15
16
17
18
19
20
21
22
23
24
25
26
27
28
29
30
31
32
33
34
35
36
37
38
39
40
41
42
43
44
45
46
47
48
49
50
51
52
53
54
55
56
57
58
59
60
61
62
63
64
65

134 the integrated areas of bound water ($T_2 = 100 \mu\text{s}-800 \mu\text{s}$) and pore water ($T_2 = 800 \mu\text{s} - 600$
135 ms) to the area of the reference ($T_2 = 600 \text{ ms}-10 \text{ s}$) [41], the volume of bound water and the
136 volume of pore water were divided by the specimen volume (calculated from Archimedes'
137 principle) to give bound water (bw) and pore water (pw) volume fractions.

138 139 *Material-level biomechanical properties*

140 Whole bone material properties, determined using 3 point bending of the femora, have been
141 previously reported [14]. Material-level properties were estimated using standard beam theory
142 equations [30]. Bone diameters were measured at the mid-diaphysis using digital calipers while
143 cross-sectional moment of inertia was measured using micro computed tomography.

144 145 *Statistical Analysis*

146 All analyses were performed using SAS software. Comparisons among the groups were made
147 using student's t-tests as the focus of this work was to independently assess high/lower turnover
148 conditions versus control. Pearson product moment correlation tests were used to assess the
149 relationship between variables across all treatments with the exception of hydration for which
150 Spearman correlations were used, as the data were not normally distributed. *A priori* α -levels
151 were set at 0.05 to determine significance.

152 153 **RESULTS**

154 *High-turnover CKD model*

155 Details about the phenotype of these animals with secondary hyperparathyroidism have been
156 previous published [14]. Briefly, measures of kidney function and PTH were both significantly
157 higher compared to normal (+200 and 2800%, respectively), indicative of active disease.
158 Trabecular bone turnover, measured by dynamic histomorphometry, was more than 4-fold

1
2
3
4
5
6
7
8
9
10
11
12
13
14
15
16
17
18
19
20
21
22
23
24
25
26
27
28
29
30
31
32
33
34
35
36
37
38
39
40
41
42
43
44
45
46
47
48
49
50
51
52
53
54
55
56
57
58
59
60
61
62
63
64
65

159 higher in compared normal; cortical porosity was more than doubled. Structural biomechanical
160 properties, ultimate load and stiffness, were both significantly lower than controls with no
161 difference in energy to fracture, a biomechanical property that is not independent of bone
162 structure [14].

163 All measured forms of collagen cross-links were significantly different compared to
164 normal. The two mature enzymatic cross-links, Pyd and Dpd were both significantly lower (-
165 21%; $p = 0.004$ and 0.02) compared to control (**Figure 1A**). There was no significant difference
166 in the Pyd/Dpd ratio. PE, an advanced glycation product, was 71% ($p = 0.001$) higher
167 compared to normal (**Figure 1B**). Pore water volume fraction within the femoral cortex was
168 higher (+46%; $p = 0.024$) while matrix bound water volume fraction was significantly lower (-
169 10%; $p = 0.04$) compared to normal animals (**Figure 1C**).

170 Ultimate stress was significantly lower than normal animals (-22%; $p=0.001$) with no
171 difference in modulus and a trend toward lower toughness (-21%; $p = 0.11$) (**Table 1**).

172 *Low-turnover CKD model*

173 Details about the phenotype of these animals, where PTH is suppressed with the administration
174 of calcium in the drinking water, have been previous published [14]. Briefly, measures of kidney
175 function were significantly higher (+150%), while PTH was significantly lower (-75%) compared
176 to normal. Trabecular bone turnover, cortical porosity, and structural properties were not
177 different from controls.

178 Levels of Pyd in the bone matrix were not different from controls, while Dpd levels were
179 significantly higher (+24%; $p = 0.002$) compared to normal (**Figure 2A**). There was no
180 significant difference in the Pyd/Dpd ratio. PE was 72% higher ($p = 0.001$ compared to normal
181 (**Figure 2B**). The NMR-derived pore water within the femoral cortex was lower (-60%; $p =$
182 0.001), and bound water was significantly higher (7%; $p = 0.04$) compared to normal animals
183 (**Figure 2C**).

1
2
3
4 185 Toughness was significantly lower than normal animals (-27%; $p = 0.005$) (**Table 1**).

5
6 186 Ultimate stress and modulus were similar to normal animals.
7
8
9 187

10 188 *Correlations*

11
12
13 189 To examine relationships between outcome measures, correlations were assessed across the
14
15 190 entire data set (controls, low turnover CKD and high turnover CKD). Kidney function (assessed
16
17 191 by BUN) was significantly correlated to PE ($R = 0.68$) (**Figure 3A**). PTH was significantly
18
19 192 correlated to several outcomes including pore water ($R = 0.81$), bound water ($R = -0.70$), pyd (-
20
21 193 0.58), Dpd ($R = -0.72$), and PE ($R = 0.46$). PE levels were negatively correlated to ultimate
22
23 194 stress and toughness ($R = -0.44$ and -0.57 , respectively) (**Figure 3B**).
24
25
26 195

27 196 **DISCUSSION**

28
29
30 197 It is becoming clear that the increased risk of skeletal fracture associated with chronic kidney
31
32 198 disease is multi-factorial and occurs due to changes in both bone quantity and quality [12, 20,
33
34 199 21, 42]. We have previously documented in an animal of progressive kidney disease, that
35
36 200 compromised biomechanical properties can be quantified at the whole bone level as well as at
37
38 201 the micro- and nano-scales [16]. These data illustrate that loss of bone mass, as has been
39
40 202 repeatedly documented in both clinical and preclinical studies, is just one piece of the CKD
41
42 203 fracture risk puzzle. Given the nano-scale changes in bone mechanical properties, our
43
44 204 laboratory has focused on measuring properties of the tissue matrix that contribute to this level
45
46 205 of mechanical integrity [16]. The results of the current work, in a preclinical animal model of
47
48 206 progressive CKD, point to modification of both collagen crosslinking and bone hydration in late
49
50 207 stage CKD. The changes in crosslinks confirm previous preclinical work in a different CKD
51
52 208 model of high turnover bone [29], while the hydration data results represent novel data and a
53
54 209 potential variable that could be used for non-invasive clinical assessment of bone quality [33,
55
56 210 43].
57
58
59
60
61
62
63
64
65

1
2
3
4
5
6
7
8
9
10
11
12
13
14
15
16
17
18
19
20
21
22
23
24
25
26
27
28
29
30
31
32
33
34
35
36
37
38
39
40
41
42
43
44
45
46
47
48
49
50
51
52
53
54
55
56
57
58
59
60
61
62
63
64
65

211 Collagen crosslinks in bone are either enzymatically-mediated (via lysyl oxidase) or non-
212 enzymatically mediated (in the form of advanced glycation end products (AGEs) such as
213 pentosidine) [22]. The predominant mature enzymatic crosslinks – pyridinoline and
214 deoxypyridinoline (also known as hydroxylslypyridinoline and lyslypyridinoline, respectively) –
215 have been shown to be associated with changes in bone mechanical properties [22]. Previous
216 work by our lab in the same animal model as the current study showed no difference in Ppd or
217 Dpd in CKD animals at 30 weeks [16]. We have documented that this animal model has rapid
218 disease progression, in high-turnover states, between 30 and 35 weeks of age [14, 15], leading
219 us to hypothesize that major changes in collagen cross-links might manifest with progression to
220 advanced disease. Although this turned out to be the case, the story is more complicated as the
221 enzymatic crosslink changes were dependent of rate turnover; high turnover groups had
222 reduced enzymatic cross-links while low turnover animals had higher than normal levels of Dpd.

223 The simplistic relationship between bone turnover and collagen crosslinks is an inverse
224 one. High bone turnover leads to lower levels of mature enzymatic crosslinks because the
225 mean tissue age is lower; while low turnover bone typically has high levels. Yet this relationship
226 model assumes that the process of collagen crosslinks formation/maturation is not disrupted.
227 Levels of lysyl oxidase, the key enzyme involved in enzymatic crosslinking, are tissue-specific.
228 Kidney levels of lysyl oxidase have been shown to be higher in CKD and this is associated with
229 increased fibrosis in renal tissue [44]. Serum measures of pyridinoline have been shown to be
230 increased in patients with end stage renal disease, and these levels were higher in patients with
231 high turnover compared to those with low turnover [45]. Yet these serum measures do not
232 provide insight into skeletal levels, as the latter are determined both the rate of
233 formation/breakdown (i.e., bone turnover) and the rate of crosslink maturation (i.e., divalent to
234 trivalent bonded). Skeletal levels of mature crosslinks have been found to be lower in patients
235 with high-turnover end stage renal disease [27], while animal models of low turnover have
236 shown reductions in bone lysyl oxidase levels [28]. Reduction in lysyl oxidase would reduce

1
2
3
4
5
6
7
8
9
10
11
12
13
14
15
16
17
18
19
20
21
22
23
24
25
26
27
28
29
30
31
32
33
34
35
36
37
38
39
40
41
42
43
44
45
46
47
48
49
50
51
52
53
54
55
56
57
58
59
60
61
62
63
64
65

237 enzymatic cross-links – although neither the clinical nor preclinical study measured both
238 enzyme and crosslinks. Unfortunately, levels of lysyl oxidase were not assessed in the current
239 work and thus definitive mechanisms underlying changes in mature cross-links cannot be
240 ascertained.

241 Clinical studies have demonstrated that non-enzymatic cross-links (pentosidine,
242 specifically) are increased in the circulation and soft tissue of patients with CKD [46]. Increased
243 oxidative stress in CKD leads to increased production of AGE, and AGEs worsen oxidative
244 stress creating a vicious cycle that is independent of blood glucose levels [47]. Skeletal levels
245 of AGEs have been shown to be elevated in a small clinical study in patients on dialysis [27].
246 Although we have recently shown that at 30 weeks of age there is no difference in skeletal
247 AGEs in our progressive CKD model, the current results show that at 35 weeks there is a
248 striking difference (>70% higher than normal). This suggests that, like the enzymatic cross-
249 links, major changes occur between 30 and 35 weeks in this animal model. More interesting is
250 that the levels of AGEs in the bone are independent of bone remodeling rate – both high and
251 low turnover models had similarly higher AGE levels compared to controls (**Figures 1B and**
252 **2B**). AGEs are typically linked to mean tissue age – since they accumulate in tissues over time
253 when mean tissue age is higher AGEs are higher. It therefore follows that, in normal situations,
254 bone with higher turnover rates will have lower AGEs compared to bone with lower turnover
255 rates. This does not seem to hold true in the setting of CKD suggesting there is some intrinsic
256 aspect of the disease that results in more AGE accumulation in bone independent of tissue age,
257 perhaps due to ongoing AGE production in CKD [47] and reduced clearance by the kidney [48].
258 We hypothesize that elevations in oxidative stress may be underlying the accumulation of AGEs
259 in this model. Thus, the severity of kidney disease may be more important than the level of
260 bone turnover for determination of skeletal AGEs. The importance of the severity of kidney
261 function is supported by a modest positive correlation between serum BUN and skeletal
262 pentosidine (R = 0.679) in the current study (**Figure 3A**).

1
2
3
4
5
6
7
8
9
10
11
12
13
14
15
16
17
18
19
20
21
22
23
24
25
26
27
28
29
30
31
32
33
34
35
36
37
38
39
40
41
42
43
44
45
46
47
48
49
50
51
52
53
54
55
56
57
58
59
60
61
62
63
64
65

263 The influence of hydration on bone mechanical properties has long been appreciated as
264 it pertains to *ex vivo* mechanical testing [30, 31]. More recently data have emerged showing
265 modulation of hydration can occur *in vivo* [34], suggesting that it could play a role in disease-
266 related bone mechanical phenotypes. The results of the current study show that in high
267 turnover disease, pore water is significantly higher, while in low turnover disease pore water is
268 lower, than normal animals. Changes in pore water track closely to changes in cortical porosity,
269 which is high in high turnover animals and low in low turnover animals at 35 weeks of age [14].
270 The changes in bound water, which have been shown to have predominant mechanical effect
271 on bone [34], were unexpected and the mechanisms through which bound water is modulated *in*
272 *vivo* remain unclear. Bound water tends to be inversely related to mineralization and at least at
273 30 weeks of age mineralization characteristics (determined by Raman spectroscopy) are not
274 different from controls [16]. It is possible that mineral has changed by week 35 in these animals
275 yet unfortunately tissue is not available for such analyses. Also, as intracortical porosity
276 increases, there is more pore water but less matrix interactions with water molecules. This is
277 confirmed in the current work by the positive correlation between pore water and porosity ($R =$
278 0.69).

279 Both AGE levels and bone hydration have been documented as having significant
280 effects on bone mechanical properties. Increasing AGE levels either *in vitro*, or *in vivo*, are
281 inversely related to bone toughness – the ability of the bone tissue to absorb energy before
282 fracture [23, 49]. Reductions in bone toughness reflect a bone that fractures more easily and in
283 a more brittle fashion [50]. Conversely to AGEs, modulating bone hydration (specifically bound
284 water) has been shown to have a positive relationship to bone toughness [34, 51]. Estimation of
285 material-level mechanical properties in the current study shows that both high and low turnover
286 disease lower bone toughness relative to normal animals, with only the lower turnover animals
287 reaching statistical significance (**Table 1**). Interestingly, these two conditions had contrasting
288 effects on pore and bound water, as well as enzymatically-mediated crosslinks. The only

1
2
3
4
5
6
7
8
9
10
11
12
13
14
15
16
17
18
19
20
21
22
23
24
25
26
27
28
29
30
31
32
33
34
35
36
37
38
39
40
41
42
43
44
45
46
47
48
49
50
51
52
53
54
55
56
57
58
59
60
61
62
63
64
65

289 common feature of the two conditions was a significant increase in levels of AGEs (pentosidine).
290 Skeletal pentosidine was negatively correlated to bone toughness ($r = -0.57$; **Figure 3B**). While
291 we cannot definitively conclude that the higher AGE levels are fully responsible for the
292 biomechanical phenotype, the results of this work suggest it is an outcome that should be a
293 primary focus in future studies.

294 In conclusion, using an animal model of progressive chronic kidney disease, we have
295 shown that both collagen crosslinking and skeletal hydration are affected in late-stage renal
296 disease. Although both of these variables are known to play roles in bone mechanical
297 properties, the data suggest that accumulation on non-enzymatic collagen crosslinks may be a
298 key change that is responsible for altering mechanical properties associated with late-stage
299 disease progression.

300

CONFLICT OF INTEREST

301 Matthew R. Allen, Christopher L. Newman, Neal Chen, Mathilde Granke, Jeffry S. Nyman, and
302 Sharon M. Moe declare they have no conflicts of interest related to this work.

304

ACKNOWLEDGEMENTS

305 This work was supported by National Institutes of Health grants AR58005 (SM), DL100093
306 (CN), AR063157 (JSN), and the Indiana Clinical Translational Science Institute grant TR000162
307 (CN). The cross-link analysis is the result of work supported with resources and the use of
308 facilities at the VA Tennessee Valley Healthcare System. All authors were involved in the
309 design, conduct and analyses of the study. The authors would like to thank Drew Brown,
310 Shannon Roy, and Kali O'Neill for technical assistance. We would also like to acknowledge the
311 late Dr. Vincent H. Gattone II (1951-2013), who was instrumental in developing this animal
312 model.
313

1
2
3
4
5
6
7
8
9
10
11
12
13
14
15
16
17
18
19
20
21
22
23
24
25
26
27
28
29
30
31
32
33
34
35
36
37
38
39
40
41
42
43
44
45
46
47
48
49
50
51
52
53
54
55
56
57
58
59
60
61
62
63
64
65

314 **FIGURE LEGENDS**

315 **Figure 1.** High-turnover CKD associated changes in skeletal collagen crosslinking and tissue
316 hydration. (A) Enzymatic collagen cross-links (pyridinoline, PYD and deoxypyridinoline, DPD)
317 were significantly lower in CKD compared to normal littermates. (B) Pentosidine, an advanced
318 glycation end product, was found in significantly higher concentrations in CKD bone compared
319 to normal. (C) Pore water fraction was significantly higher and bound water fraction significantly
320 lower in CKD animals compared to normal. * $p < 0.05$ compared to normal animals.

321
322 **Figure 2.** Low-turnover CKD associated changes in skeletal collagen crosslinking and tissue
323 hydration. (A) The enzymatic collagen cross-link (deoxypyridinoline, DPD) was significantly
324 higher than normal in low-turnover disease; pyridinoline, PYD was unaffected. (B) Pentosidine,
325 an advanced glycation end product, was found in significantly higher concentrations in CKD
326 bone compared to normal. (C) Pore water fraction was significantly lower and bound water
327 fraction significantly higher in CKD animals compared to normal. * $p < 0.05$ compared to normal
328 animals.

329 **Figure 3.** Correlations between skeletal pentosidine levels and kidney function (A) and
330 mechanical properties (B). As both high and low turnover CKD models were shown to have
331 higher pentosidine levels compared to normal we explored the relationship between kidney
332 function and pentosidine. This relationship was statistically significant ($r = 0.68$, $p < 0.001$).
333 Given the known role of pentosidine in modulation of mechanical properties we also explored
334 the relationship between pentosidine and bone toughness (B). This relationship was statistically
335 significant ($r = -0.57$, $p = 0.002$).

1
2
3
4
5
6
7
8
9
10
11
12
13
14
15
16
17
18
19
20
21
22
23
24
25
26
27
28
29
30
31
32
33
34
35
36
37
38
39
40
41
42
43
44
45
46
47
48
49
50
51
52
53
54
55
56
57
58
59
60
61
62
63
64
65

337
338 Table 1. Femoral diaphysis morphology and calculated material-level biomechanical properties
339

	Normal	High turnover CKD	Low turnover CKD
Bone diameter, mm	3.7 ± 0.2	3.6 ± 0.2	3.7 ± 0.1
Porosity, %	0.1 ± 0.1	4.1 ± 5.4 *	0.5 ± 0.2 *
Cross-sectional moment of inertia, mm ⁴	10.1 ± 1.5	8.56 ± 0.9 *	11.1 ± 1.4
Ultimate stress, MPa	180 ± 17	140 ± 25 *	176 ± 27
Modulus, MPa	6777 ± 831	6609 ± 750	6701 ± 880
Toughness, MJ/m ³	5.3 ± 1.1	4.2 ± 1.8	3.9 ± 0.7 *

340
341 Values are presented as mean ± standard deviation.
342 * p < 0.05 versus normal controls.

1
2
3
4 366 REFERENCES

- 5 367
6 368 1. Moe S, Drüeke T, Cunningham J, et al. (2006) Definition, evaluation, and classification of
7 369 renal osteodystrophy: a position statement from Kidney Disease: Improving Global
8 370 Outcomes (KDIGO). In: *Kidney Int.* pp 1945–1953
- 10
11 371 2. Nickolas TL, McMahon DJ, Shane E (2006) Relationship between moderate to severe kidney
12 372 disease and hip fracture in the United States. *J Am Soc Nephrol* 17:3223–3232.
- 13
14 373 3. Ensrud KE, Lui L-Y, Taylor BC, et al. (2007) Renal function and risk of hip and vertebral
15 374 fractures in older women. *Arch Intern Med* 167:133–139.
- 16
17 375 4. Anderson S, Halter JB, Hazzard WR, et al. (2009) Prediction, Progression, and Outcomes of
18 376 Chronic Kidney Disease in Older Adults. *Journal of the American Society of Nephrology*
19 377 20:1199–1209.
- 20
21
22 378 5. Jamal SA, West SL, Miller PD (2011) Fracture risk assessment in patients with chronic kidney
23 379 disease. *Osteoporos Int* 23:1191–1198.
- 24
25 380 6. Nitsch D, Mylne A, Roderick PJ, et al. (2009) Chronic kidney disease and hip fracture-related
26 381 mortality in older people in the UK. *Nephrol Dial Transplant* 24:1539–1544.
- 27
28 382 7. Fusaro M, Gallieni M, Jamal SA (2013) Fractures in chronic kidney disease: neglected,
29 383 common, and associated with sickness and death. 85:20–22.
- 30
31
32 384 8. Negrea LA (2012) Biochemical Abnormalities in Chronic Kidney Disease–Mineral Bone
33 385 Disease. *Clinic Rev Bone Miner Metab* 10: 149-162.
- 34
35 386 9. Kiattisunthorn K, Moe SM (2011) Chronic Kidney Disease-Mineral Bone Disorder: Definitions
36 387 and Rationale for a Systemic Disorder. *Clinic Rev Bone Miner Metab* 10:119–127.
- 37
38 388 10. Ott SM (2009) Bone histomorphometry in renal osteodystrophy. *Semin Nephrol* 29:122–132.
- 39
40 389 11. Terpstra AM, Kalkwarf HJ, Shults J, et al. (2012) Bone Density and Cortical Structure after
41 390 Pediatric Renal Transplantation. *Journal of the American Society of Nephrology* 23:715–
42 391 726.
- 43
44
45 392 12. Nickolas TL, Stein EM, Dworakowski E, et al. (2013) Rapid cortical bone loss in patients
46 393 with chronic kidney disease. *J Bone Miner Res* 28:1811–1820.
- 47
48 394 13. Miller MA, Chin J, Miller SC, Fox J (1998) Disparate effects of mild, moderate, and severe
49 395 secondary hyperparathyroidism on cancellous and cortical bone in rats with chronic renal
50 396 insufficiency. *Bone* 23:257–266.
- 51
52
53 397 14. Moe SM, Chen NX, Newman CL, et al. (2014) A Comparison of Calcium to Zoledronic Acid
54 398 for Improvement of Cortical Bone in an Animal Model of CKD. *J Bone Miner Res* 29:902–
55 399 910.
- 56
57 400 15. Allen MR, Chen NX, Gattone VH, et al. (2012) Skeletal effects of zoledronic acid in an
58 401 animal model of chronic kidney disease. *Osteoporos Int* 24:1471–1481.
- 59
60
61
62
63
64
65

- 1
2
3
4 402 16. Newman CL, Moe SM, Chen NX, et al. (2014) Cortical Bone Mechanical Properties Are
5 403 Altered in an Animal Model of Progressive Chronic Kidney Disease. PLoS ONE 9:e99262.
6
- 7 404 17. Iwamoto J, Seki A, Sato Y, Matsumoto H (2011) Vitamin K2 Improves Renal Function and
8 405 Increases Femoral Bone Strength in Rats with Renal Insufficiency. Calcif Tissue Int 90:50–
9 406 59.
- 10
11 407 18. Moe SM, Radcliffe JS, White KE, et al. (2011) The pathophysiology of early-stage chronic
12 408 kidney disease-mineral bone disorder (CKD-MBD) and response to phosphate binders in
13 409 the rat. J Bone Miner Res 26:2672–2681.
- 14
15 410 19. Seeman E (2006) Bone quality--the material and structural basis of bone strength and
16 411 fragility. New England Journal of Medicine 354: 2250-61.
- 17
18 412 20. Malluche HH, Porter DS, Monier-Faugere MC, et al. (2012) Differences in Bone Quality in
19 413 Low- and High-Turnover Renal Osteodystrophy. Journal of the American Society of
20 414 Nephrology 23:525–532.
- 21
22 415 21. Malluche HH, Porter DS, Pienkowski D (2013) Evaluating bone quality in patients with
23 416 chronic kidney disease Nat Rev Nephrol 9: 671-680.
- 24
25 417 22. Viguet-Carrin S, Garnero P, Delmas PD (2005) The role of collagen in bone strength.
26 418 Osteoporos Int 17:319–336.
- 27
28 419 23. Vashishth D, Gibson GJ, Khoury JI, et al. (2001) Influence of nonenzymatic glycation on
29 420 biomechanical properties of cortical bone. Bone 28:195–201.
- 30
31 421 24. Wang X, Bank RA, TeKoppele JM, Agrawal CM (2001) The role of collagen in determining
32 422 bone mechanical properties. J Orthop Res 19:1021–1026.
- 33
34 423 25. John D. Currey (2003) Role of collagen and other organics in the mechanical properties of
35 424 bone. Osteoporos Int 14 Suppl 5:S29–36.
- 36
37 425 26. Oxlund H, Barckman M, Ørtoft G, Andreassen TT (1995) Reduced concentrations of
38 426 collagen cross-links are associated with reduced strength of bone. Bone 17:S365–S371.
- 39
40 427 27. Mitome J, Yamamoto H, Saito M, et al. (2011) Nonenzymatic Cross-Linking Pentosidine
41 428 Increase in Bone Collagen and Are Associated with Disorders of Bone Mineralization in
42 429 Dialysis Patients. Calcif Tissue Int 88:521–529.
- 43
44 430 28. Aoki C, Uto K, Honda K, et al. (2013) Advanced glycation end products suppress lysyl
45 431 oxidase and induce bone collagen degradation in a rat model of renal osteodystrophy.
46 432 93:1170–1183.
- 47
48 433 29. Iwasaki Y, Kazama JJ, Yamato H, Fukagawa M (2011) Changes in chemical composition of
49 434 cortical bone associated with bone fragility in rat model with chronic kidney disease. Bone
50 435 48:1260–1267.
- 51
52 436 30. Turner CH, Burr DB (1993) Basic biomechanical measurements of bone: a tutorial. Bone
53 437 14:595–608.

- 1
2
3
4 438 31. Dempster WT, Liddicoat RT (1952) Compact bone as a non-isotropic material. *Am J Anat*
5 439 91:331–362.
6
7 440 32. Nyman JS, Gorochow LE, Adam Horch R, et al. (2013) Partial removal of pore and loosely
8 441 bound water by low-energy drying decreases cortical bone toughness in young and old
9 442 donors. *Journal of the Mechanical Behavior of Biomedical Materials* 22:136–145.
10
11 443 33. Techawiboonwong A, Song HK, Leonard MB, Wehrli FW (2008) Cortical Bone Water: In
12 444 Vivo Quantification with Ultrashort Echo-Time MR Imaging. *Radiology* 248:824–833.
13
14
15 445 34. Gallant MA, Brown DM, Hammond M, et al. (2014) Bone cell-independent benefits of
16 446 raloxifene on the skeleton: A novel mechanism for improving bone material properties. *Bone*
17 447 61:191–200.
18
19 448 35. Anumula S, Wehrli SL, Magland J, et al. (2010) Ultra-short echo-time MRI detects changes
20 449 in bone mineralization and water content in OVX rat bone in response to alendronate
21 450 treatment. *Bone* 46:1391–1399.
22
23
24 451 36. Moe SM, Chen NX, Seifert MF, et al. (2009) A rat model of chronic kidney disease-mineral
25 452 bone disorder. *Kidney Int* 75:176–184.
26
27 453 37. Cowley BD, Grantham JJ, Muessel MJ, et al. (1996) Modification of disease progression in
28 454 rats with inherited polycystic kidney disease. *YAJKD* 27:865–879.
29
30 455 38. Cowley BD, Gudapaty S, Kraybill AL, et al. (1993) Autosomal-dominant polycystic kidney
31 456 disease in the rat. *Kidney Int* 43:522–534.
32
33
34 457 39. Horch RA, Wilkens K, Gochberg DF, Does MD (2010) RF coil considerations for short-T2
35 458 MRI. *Magnetic Resonance Medicine* 64:1652–1657.
36
37 459 40. Horch RA, Nyman JS, Gochberg DF, et al. (2010) Characterization of 1H NMR signal in
38 460 human cortical bone for magnetic resonance imaging. *Magnetic Resonance Medicine*
39 461 64:680–687.
40
41 462 41. Horch RA, Gochberg DF, Nyman JS, et al. (2011) Non-invasive predictors of human cortical
42 463 bone mechanical properties: T(2)-discriminated H NMR compared with high resolution X-
43 464 ray. *PLoS ONE* 6:e16359.
44
45 465 42. Leonard MB (2009) A Structural Approach to Skeletal Fragility in Chronic Kidney Disease.
46 466 *Semin Nephrol* 29:133–143.
47
48 467 43. Manhard MK, Horch RA, Harkins KD, et al. (2014) Validation of quantitative bound- and
49 468 pore-water imaging in cortical bone. *Magn Reson Med* 71:2166–2171.
50
51 469 44. Di Donato A, Ghiggeri GM, Di Duca M, et al. (1997) Lysyl Oxidase Expression and Collagen
52 470 Cross-Linking during Chronic Adriamycin Nephropathy. *Nephron* 76:192–200.
53
54 471 45. Ureña P, Ferreira A, Kung VT, et al. (1995) Serum pyridinoline as a specific marker of
55 472 collagen breakdown and bone metabolism in hemodialysis patients. *J Bone Miner Res*
56 473 10:932–939.
57
58
59
60
61
62
63
64
65

1
2
3
4
5
6
7
8
9
10
11
12
13
14
15
16
17
18
19
20
21
22
23
24
25
26
27
28
29
30
31
32
33
34
35
36
37
38
39
40
41
42
43
44
45
46
47
48
49
50
51
52
53
54
55
56
57
58
59
60
61
62
63
64
65

474 46. Suliman ME, Heimbürger O, Bárány P, et al. (2003) Plasma pentosidine is associated with
475 inflammation and malnutrition in end-stage renal disease patients starting on dialysis
476 therapy. *J Am Soc Nephrol* 14:1614–1622.

477 47. Mallipattu SK, Uribarri J (2014) Advanced glycation end product accumulation. *Current*
478 *Opinion in Nephrology and Hypertension* 6: 547-554.

479 48. Miyata T, Ueda Y, Horie K, et al. (1998) Renal catabolism of advanced glycation end
480 products: the fate of pentosidine. *Kidney Int* 53:416–422.

481 49. Tang SY, Allen MR, Phipps R, et al. (2009) Changes in non-enzymatic glycation and its
482 association with altered mechanical properties following 1-year treatment with risedronate
483 or alendronate. *Osteoporos Int* 20:887–894.

484 50. Burr D (2011) Why bones bend but don't break. *11*: 270-285.

485 51. Bae WC, Chen PC, Chung CB, et al. (2012) Quantitative ultrashort echo time (UTE) MRI of
486 human cortical bone: Correlation with porosity and biomechanical properties. *J Bone Miner*
487 *Res* 27:848–857.

488
489
490

Figure 1
[Click here to download high resolution image](#)

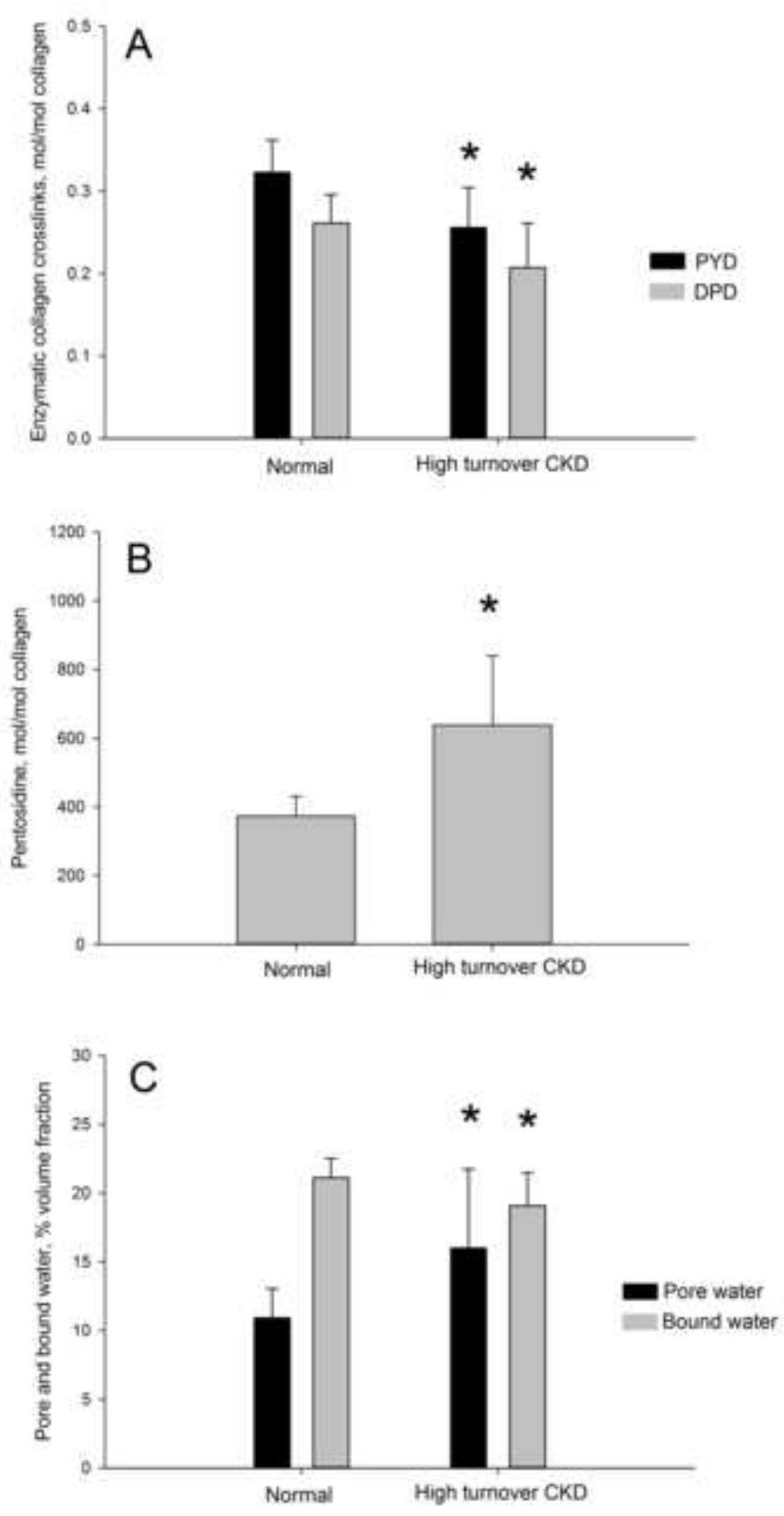


Figure 2

[Click here to download high resolution image](#)

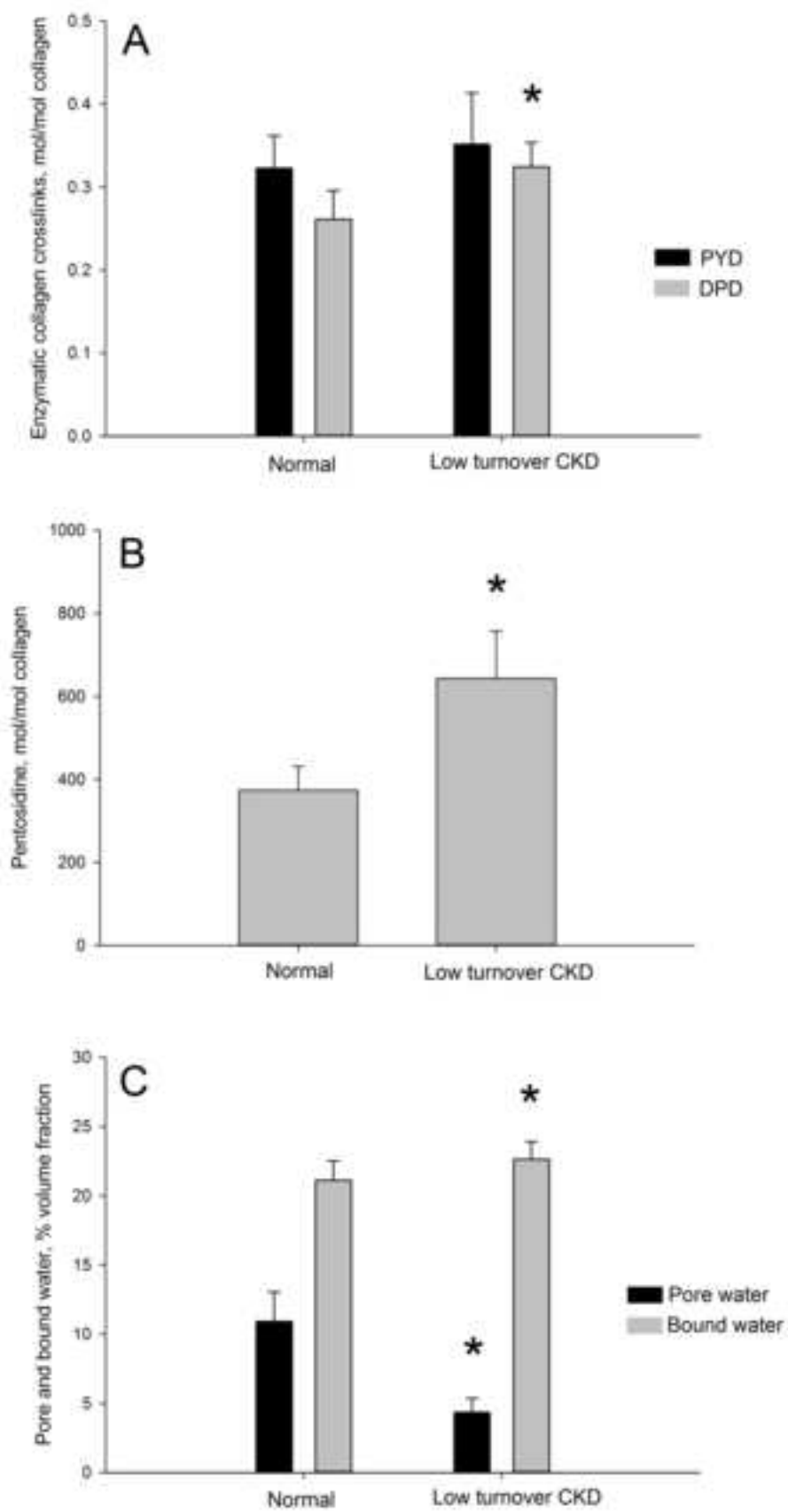


Figure 3

[Click here to download high resolution image](#)

